THE JOURNAL OF BIOLOGICAL CHEMISTRY VOL. 285, NO. 6, pp. 3592–3599, February 5, 2010
Printed in the U.S.A.

Quantitative Characterization of Heparin Binding to Tau Protein

IMPLICATION FOR INDUCER-MEDIATED TAU FILAMENT FORMATION[*][S]

Received for publication, June 18, 2009, and in revised form, December 1, 2009 Published, JBC Papers in Press, December 3, 2009, DOI 10.1074/jbc.M109.035691

Hai-Li Zhu[‡], Cristina Fernández[§], Jun-Bao Fan[‡], Frank Shewmaker[§], Jie Chen[‡], Allen P. Minton[§], and Yi Liang[‡1]

From the [‡]State Key Laboratory of Virology, College of Life Sciences, Wuhan University, Wuhan 430072, China and the [§]Laboratory of Biochemistry and Genetics, NIDDK, National Institutes of Health, Bethesda, Maryland 20892

Neurofibrillary tangles, principally composed of bundles of filaments formed by the microtubule-associated protein Tau, are a hallmark of a group of neurodegenerative diseases such as Alzheimer disease. Polyanionic cofactors such as heparin can induce Tau filament formation *in vitro*. Here we quantitatively characterize the interaction between recombinant human Tau fragment $Tau_{244-372}$ and heparin (average molecular mass = 7 kDa) as well as heparin-induced fibril formation by using static light scattering, isothermal titration calorimetry, turbidity assays, and transmission electron microscopy. Our data clearly show that at physiological pH, heparin 7K, and human $Tau_{244-372}$ form a tight 1:1 complex with an equilibrium association constant exceeding 10^6 M^{-1} under reducing conditions, triggering Tau fibrillization. In the absence of dithiothreitol, heparin shows a moderate binding affinity (10^5 M^{-1}) to $Tau_{244-372}$, similarly triggering Tau fibrillization. Further fibrillization kinetics analyses show that the lag time appears to be approximately invariant up to a molar ratio of 2:1 and then increases at larger ratios of heparin/Tau. The maximum slope representing the apparent rate constant for fibril growth increases sharply with substoichiometric ratios of heparin/Tau and then decreases to some extent with ratios of >1:1. The retarding effect of heparin in excess is attributed to the large increase in ionic strength of the medium arising from free heparin. Together, these results suggest that the formation of the 1:1 complex of Tau monomer and heparin plays an important role in the inducer-mediated Tau filament formation, providing clues to understanding the pathogenesis of neurodegenerative diseases.

Microtubule-associated protein Tau is the major protein subunit of neurofibrillary tangles, one of the major neuropathological hallmarks of a group of neurodegenerative diseases such as Alzheimer disease (1, 2). Neurofibrillary tangles are mainly composed of bundles of Tau in the form of paired helical filaments, straight filaments, or twisted ribbons (3). Because the accumulation of Tau aggregates correlates well with nerve cell loss and the severity of dementia, formation of a neurofibrillary tangle is considered to be involved in the pathways leading to neuronal death (4–6), and the characterization of factors involved in Tau fibrillization is of great importance to clarify the etiology of such neurodegenerative diseases.

Tau is among one of the largest proteins without recognizable secondary structure and adopts a natively unfolded structure in solution (7). It binds to microtubules through four repeat domains in its C-terminal part (8). The repeat domain of Tau forms the core of paired helical filaments in Alzheimer disease and also assembles more readily than full-length Tau into *bona fide* paired helical filaments *in vitro* (9, 10).

To mimic Tau fibrillization *in vivo*, polyanionic cofactors such as heparin have been used to induce Tau filament formation *in vitro* (1, 11–14). It has been shown that Tau and heparan sulfate (HS)[2] coexist in nerve cells with overt neurofibrillary lesion (12). The molecular basis for such an inducement process remains unknown. However, the discovery that other polyanions such as RNA (15) or arachidonic acid (16) can also cause Tau filament formation indicates that Tau aggregation is rather influenced by electrostatics than by the precise nature of the negatively charged polymers (17). The kinetics for inducer-mediated Tau filament formation can be characterized by a lag period, followed by a period of exponential growth and an asymptotic approach to equilibrium (13, 18–20). The filamentous structures induced by heparin are structurally similar to those found in Alzheimer disease (1), and thus heparin-induced Tau aggregation serves as a good model for pathological Tau fibrillization.

In the present study, we quantitatively characterized the interaction between recombinant human Tau fragment $Tau_{244-372}$ and heparin as well as heparin-induced fibril formation of $Tau_{244-372}$ by using several biophysical methods, such as static light scattering, isothermal titration calorimetry (ITC), turbidity assays, and transmission electron microscopy. Our data demonstrated that at physiological pH and temperature, human $Tau_{244-372}$ did form a 1:1 complex with heparin. Heparin shows a strong binding affinity to $Tau_{244-372}$ in the presence of dithiothreitol (DTT), triggering Tau fibrillization under such reducing conditions.

* This work was supported by National Key Basic Research Foundation of China Grant 2006CB910301, National Natural Science Foundation of China Grants 30770421 and 30970599, and Chinese 111 Project Grant B06018. This work was also supported in part by National Institutes of Health grants through the Intramural Research Program of the NIDDK.

[S] The on-line version of this article (available at http://www.jbc.org) contains supplemental Fig. S1.

[1] Recipient of a visiting appointment in the Laboratory of Biochemistry and Genetics, NIDDK. To whom correspondence should be addressed. Tel.: 86-27-6875-4902; Fax: 86-27-6875-4902; E-mail: liangyi@whu.edu.cn.

[2] The abbreviations used are: HS, heparan sulfate; DTT, dithiothreitol; ITC, isothermal titration calorimetry.

EXPERIMENTAL PROCEDURES

Materials—Heparin (average molecular mass of 7 kDa) was obtained from Sigma-Aldrich. DTT was obtained from Ameresco (Solon, OH). All other chemicals used were made in China and were of analytical grade. All of the reagent solutions were prepared in 10 mM HEPES buffer (pH 7.4) containing 100 mM NaCl.

Plasmids and Proteins—The cDNA encoding human Tau fragment $Tau_{244-372}$ was amplified using the plasmid for human Tau40 (kindly provided by Dr. Michel Goedert) as a template. The PCR-amplified $Tau_{244-372}$ was subcloned into pRK172 vector. Recombinant $Tau_{244-372}$ was expressed in *Escherichia coli* and purified to homogeneity by SP Sepharose chromatography as described (21). Purified Tau protein was analyzed by SDS-PAGE with one band. The concentration of human Tau fragment was determined according to its absorbance at 214 nm with a standard calibration curve drawn by bovine serum albumin.

Turbidity Assays—Samples of 160 μM $Tau_{244-372}$ were incubated at 37 °C in 10 mM HEPES buffer (pH 7.4) containing heparin at different concentrations (20–640 μM) and 100 mM NaCl in the presence and absence of 1 mM DTT or in 10 mM HEPES buffer (pH 7.4) containing 160 μM heparin and NaCl at different concentrations (0–500 mM) in the presence of 1 mM DTT. The solutions with a volume of 250 μl were placed into a well of a 96-well plate followed by monitoring the turbidity at 350 nm using a SpectraMax 190 microplate reader (Molecular Devices, Sunnyvale, CA). Each sample was run in triplicate or quadruplicate. The profile of absorbance *versus* time was analyzed as follows. A seventh order polynomial was fitted to all of the data $\{t, A_{350}\}$from replicates at each heparin concentration. The maximum slope of the best fit polynomial $(dP/dt)_{max}$, the value of t corresponding to maximum slope of the polynomial t^*, and the value of the polynomial at this time $P(t^*)$ were evaluated. A straight line with slope $(dP/dt)_{max}$ was drawn through $\{t^*, P(t^*)\}$, and the value of t at which this line crosses the t axis ($P = 0$) is designated the lag time.

Transmission Electron Microscopy—The formation of filaments by human Tau fragment was confirmed by electron microscopy of negatively stained samples. Sample aliquots of 10 μl were placed on copper grids and left at room temperature for 1–2 min, rinsed with H_2O twice, and then stained with 2% (w/v) uranyl acetate for another 1–2 min. The stained samples were examined using an H-8100 transmission electron microscope (Hitachi, Tokyo, Japan) operating at 100 kV or an FEI Morgagni transmission electron microscope operating at 80 kV.

Isothermal Titration Calorimetry—ITC experiments on the interaction of heparin with $Tau_{244-372}$ in the absence of DTT were carried out at 37.0 °C using a VP-ITC titration calorimetry (MicroCal, Northampton, MA). Freshly purified wild-type $Tau_{244-372}$ and heparin were thoroughly dialyzed against 10 mM HEPES buffer (pH 7.4) containing 100 mM NaCl. A solution of 40 μM Tau protein was loaded into the sample cell (1.43 ml), and a solution of 500 μM heparin was placed in the injection syringe (280 μl). A titration experiment consisted of 13 consecutive injections of 20-μl volume and 40-s duration each, with a 4-min interval between injections, and the 14th injection of 20-μl volume and 40-s duration, with an 8-h interval. Dilution heat of heparin was measured by injecting heparin solution into buffer alone and was subtracted from the experimental curves prior to data analysis. The resulting data (injections 1–13) were fitted to a single set of identical sites model using the MicroCal ORIGIN software supplied with the instrument, and the standard molar enthalpy change for the binding, $\Delta_b H^0_m$, the binding constant, K_b, and the binding stoichiometry, n, were thus obtained. The standard molar free energy change, $\Delta_b G^0_m$, and the standard molar entropy change, $\Delta_b S^0_m$, for the binding reaction were calculated by the fundamental equations of thermodynamics (22).

$$\Delta_b G^0_m = -RT\ln K_b \quad \text{(Eq. 1)}$$

$$\Delta_b S^0_m = (\Delta_b H^0_m - \Delta_b G^0_m)/T \quad \text{(Eq. 2)}$$

Calorimetric data of injection 14 was integrated of the heat power peak of the reaction.

Composition Gradient Static Light Scattering—$Tau_{244-372}$ and heparin were thoroughly dialyzed against 10 mM HEPES buffer (pH 7.4) containing 100 mM NaCl and 1 mM DTT. Immediately before light scattering measurement, both protein and heparin solutions were filtered through a 0.02-μm filter (Anotop 10 Plus, Whatman) and centrifuged at 5000 rpm and 4 °C for 30 min to remove microscopic bubbles. The concentration of $Tau_{244-372}$ in solution A ($w_{A,load}$) and the concentration of heparin in solution B ($w_{B,load}$), determined in an Optilab rEX differential refractometer (Wyatt, Santa Barbara, CA), were 0.55 and 0.42 g/liter, respectively. The specific refractive increment of Tau (A in equations below) is $d\tilde{n}/dw_A = 0.185$ cm^3/g (23). The specific refractive increment of heparin (B in equations below) was determined experimentally. A calibration curve of refractive index *versus* heparin concentration was constructed, and the best fit value of the slope $d\tilde{n}/dw_B = 0.126$ cm^3/g is in agreement with the published values (23, 24). A composition gradient was created using the Calypso system (Wyatt, Santa Barbara, CA), in which the fraction of solution A (f_A) is decreased from 1 to 0 in steps of 0.08, and the total concentrations of Tau (A) and heparin (B) in each of these mixtures is given by the following equations.

$$w_{A,tot} = f_A w_{A,load} \quad \text{(Eq. 3)}$$

$$w_{B,tot} = (1 - f_A) w_{B,load} \quad \text{(Eq. 4)}$$

These solution mixtures were pumped in sequence into parallel flow cells in which the static light scattering intensity and refractive index of each mixture were measured simultaneously in a DAWN-EOS light scattering photometer (Wyatt) and an Optilab rEX differential refractometer (Wyatt). The raw data obtained from each instrument were respectively converted into values of the normalized scattering intensity R/K_{opt} and f_A as described (25, 26).

The equilibrium constant for formation of a 1:1 complex of Tau (A) and heparin (B) is defined as follows,

$$K_{AB} = \frac{c_{AB}}{c_A c_B} \quad \text{(Eq. 5)}$$

where c_{AB}, c_A, and c_B, respectively, denote the molar concen-

trations at equilibrium of the complex, free A, and free B. The conservation of mass is given by the following,

$$c_{A,tot} = \frac{w_{A,tot}}{M_A} = c_A + K_{AB}c_A c_B \quad \text{(Eq. 6)}$$

$$c_{B,tot} = \frac{w_{B,tot}}{M_B} = c_B + K_{AB}c_A c_B \quad \text{(Eq. 7)}$$

where $w_{A,tot}$ and $w_{B,tot}$, respectively, denote the total w/v concentrations of Tau and heparin, and M_A and M_B, respectively, denote the molar masses of Tau and heparin. Given the values of $w_{A,tot}$, $w_{B,tot}$, M_A, M_B, and K_{AB}, Equations 5–7 may be solved analytically to yield the equilibrium values of c_A, c_B, and c_{AB}.

The normalized scattering intensity is given by the following equations (27).

$$\frac{R}{K^o_{opt}} = \sum_i \left(\frac{d\tilde{n}}{dw_i}\right)^2 M_i^2 c_i \quad \text{(Eq. 8)}$$

$$K^o_{opt} = \frac{4\pi^2 \tilde{n}_0^2}{\lambda_0^4 N_A} \quad \text{(Eq. 9)}$$

In the above equations, $d\tilde{n}/dw_i$, M_i, and c_i, respectively, denote the specific refractive increment, molecular weight, and molar concentration of the ith scattering species, $\tilde{n}_0$ is the refractive index of buffer, λ_0 is the wavelength in vacuum of incident light (here 690 nm), and N_A is Avogadro's number. To facilitate modeling of scattering in mixtures containing scattering species of significantly different refractive increment, we scale the above equations as follows. We define a new optical constant,

$$K_{opt} = \frac{K^0_{opt}}{(d\tilde{n}/dw_{protein})^2} \quad \text{(Eq. 10)}$$

where $d\tilde{n}/dw_{protein}$ is set equal to the average for polypeptides, 0.185 cm^3/g (23). Then Equation 3 may be rewritten as follows.

$$\frac{R}{K_{opt}} = \sum_i G_i^2 M_i^2 c_i \quad \text{(Eq. 11)}$$

$$G_i = \frac{d\tilde{n}/dw_i}{d\tilde{n}/dw_{protein}} \quad \text{(Eq. 12)}$$

G_i^2 is thus a measure of the scattering power of a given substance relative to that of protein. The specific refractive increments of Tau (A) and heparin (B) are as follows: $d\tilde{n}/dw_A$ = 0.185 cm^3/g (23); $d\tilde{n}/dw_B$ = 0.126 cm^3/g. The refractive increment of the 1:1 complex AB is a mass average (25).

$$\frac{d\tilde{n}}{dw_{AB}} = \frac{M_A(d\tilde{n}/dw_A) + M_B(d\tilde{n}/dw_B)}{M_{AB}} \quad \text{(Eq. 13)}$$

Thus $G_A = 1$, $G_B = 0.681$, and $G_{AB} = (M_A G_A + M_B G_B)/M_{AB}$.

The experimentally determined dependence of R/K_{opt} upon f_A was modeled using Equations 3–7 to calculate the equilibrium values of c_A, c_B, and c_{AB} and then using Equation 11 with the values of G_A, G_B, and G_{AB} given above to calculate R/K_{opt}.

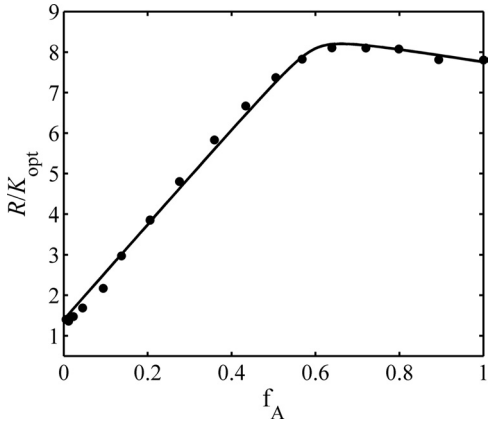

FIGURE 1. **Light scattering measurements of the binding of heparin to $Tau_{244-372}$ in the presence of DTT and at 37.0 °C.** Shown is the experimentally measured composition dependence of light scattering intensity (*solid circles*), plotted with dependence calculated as described in text using the following best fit parameter values and 95% confidence limits of estimate: M_A = 14,100 ± 700 g mol^{-1}; M_B = 7200 ± 800 g mol^{-1}; log K_{AB} = 6.5 (−1, + indeterminate).

The values of M_A, M_B, and $\log_{10} K_{AB}$ were allowed to vary to achieve a best fit via nonlinear least squares.

RESULTS

Interaction between Tau and Heparin under Reducing Conditions—The experimentally measured dependence of R/K_{opt} on f_A is plotted in Fig. 1. The dependence calculated using Equation 13 with the best fit parameter values given below is plotted together with the data. Here we quantitatively characterize the interaction between recombinant human Tau fragment $Tau_{244-372}$ and heparin in the presence of DTT using static light scattering. The best fit parameter values with 95% confidence limits of estimate were: M_A = 14,100 ± 700 g mol^{-1}; M_B = 7200 ± 800 g mol^{-1}; log K_{AB} = 6.5 (−1, + indeterminate). Our data clearly indicated that at physiological pH, heparin and human $Tau_{244-372}$ form a tight 1:1 complex with an equilibrium association constant exceeding 10^6 M^{-1} under reducing conditions.

Interaction between Tau and Heparin under Oxidative Conditions—ITC provides a direct route to the complete thermodynamic characterization of noncovalent, equilibrium interactions (28, 29), and DTT concentrations as low as 1 mM can cause severe base-line artifacts caused by background oxidation during the titration. Therefore ITC was used to measure the binding affinity of heparin to Tau protein in the absence of DTT. ITC profiles for the binding of heparin 7K to wild-type $Tau_{244-372}$ at 37.0 °C in 10 mM HEPES buffer (pH 7.4) containing 100 mM NaCl are shown in Fig. 2. Fig. 2*A* shows the raw ITC curve resulting from the injections of heparin into a solution of wild-type $Tau_{244-372}$. The titration curve shows that heparin binding to $Tau_{244-372}$ is exothermic, resulting in negative peaks in the plots of power *versus* time. Fig. 2*B* shows the plot of the heat evolved per mol of heparin added, corrected for the heat of heparin dilution, against the molar ratio of heparin to $Tau_{244-372}$. The thermodynamic parameters for the binding between heparin and $Tau_{244-372}$ ($\Delta_b H^0_m = -1.44 \pm 0.12$ kcal mol^{-1}, n = 1.08 ± 0.05, $K_b = (4.05 \pm 1.44) \times 10^5$ M^{-1}, $\Delta_b S^0_m$ = 30.28 ± 1.08 cal mol^{-1} K^{-1}, and $\Delta_b G^0_m = -7.95 \pm 0.22$ kcal mol^{-1}) were

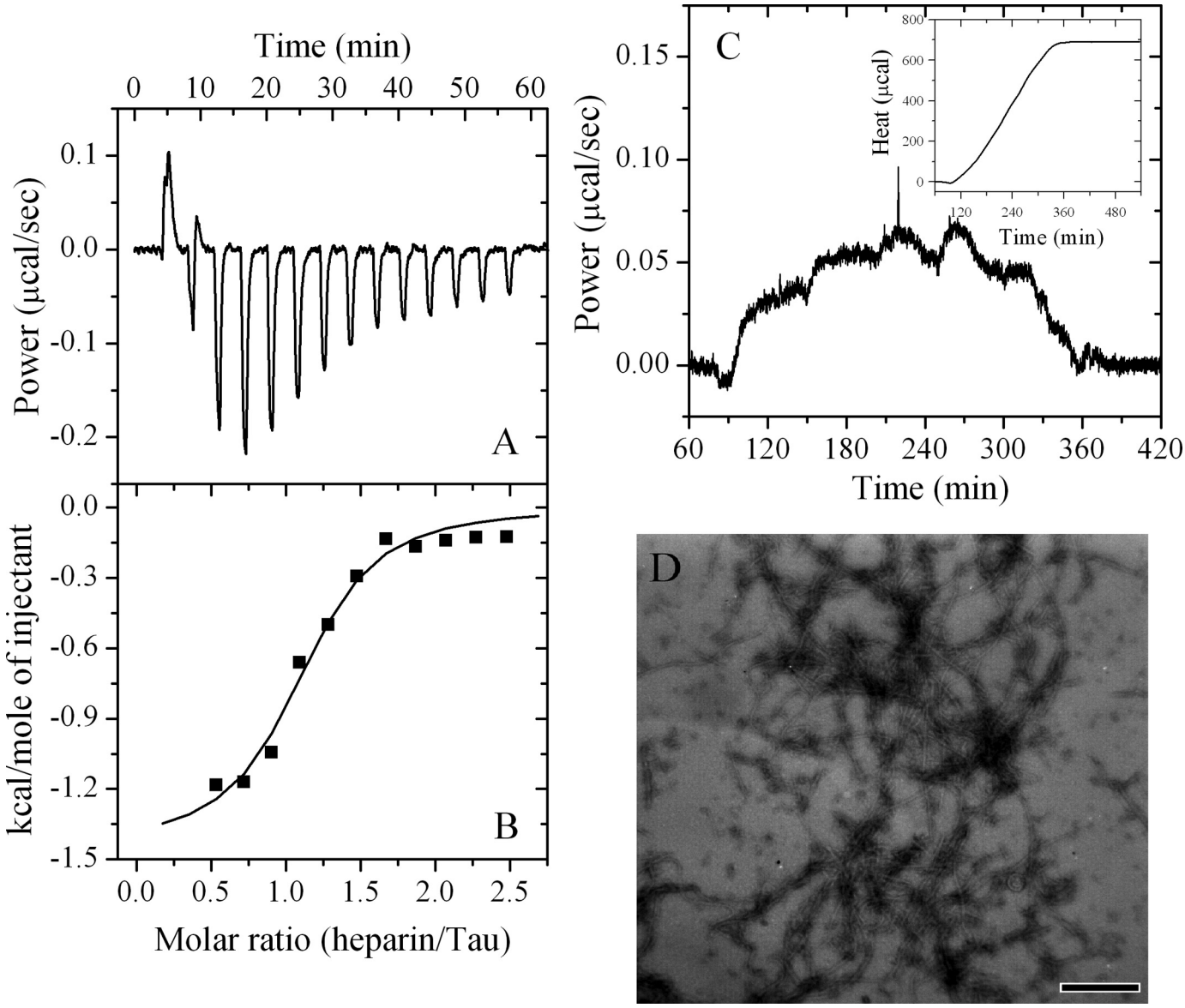

FIGURE 2. **ITC measurements of the binding of heparin to $Tau_{244-372}$ and the fibrillation of $Tau_{244-372}$ induced by heparin at 37.0 °C.** *A* represents typical calorimetric titration of $Tau_{244-372}$ (40 μM) with heparin (500 μM) in the absence of DTT. *B* shows the plots of the heat evolved (kcal) per mol of heparin added, corrected for the heat of heparin, against the molar ratio of heparin to $Tau_{244-372}$. The data (*solid squares*) were fitted to a single set of identical sites model, and the *solid line* represented the best fit. *C* represents typical calorimetric curve for the fibrillation of $Tau_{244-372}$ induced by heparin as a function of time following the binding of heparin to $Tau_{244-372}$, and the *inset* shows the heat effect of the fibrillation of $Tau_{244-372}$. *D* represents the transmission electron micrographs of $Tau_{244-372}$ fibrils formed in the calorimeter cell. The *scale bar* represents 200 nm.

obtained by fitting the data to a single set of identical sites model, indicating that one heparin bound to one $Tau_{244-372}$ with a moderate affinity in the absence of DTT. The formation of the heparin-Tau complex was driven by a large favorable entropy increase with a small favorable enthalpy increase under such oxidative conditions. Our data clearly indicated that at physiological pH, heparin and human $Tau_{244-372}$ formed a 1:1 complex with an equilibrium association constant of approximately 10^5 M^{-1} under oxidative conditions.

Heparin-mediated Tau Filament Formation under Reducing Conditions—$Tau_{244-372}$ was incubated with various concentrations of heparin in the presence of 1 mM DTT and monitored by turbidity assays. Fig. 3 shows the dependence of turbidity changes for $Tau_{244-372}$ filament formation at 37.0 °C on the molar ratio of heparin to Tau protein. The molar ratio of heparin to Tau was 1:8, 1:6, 1:4, 1:2, 1:1, 2:1, and 4:1, respectively. The kinetic curves were analyzed as described above (Fig. 3), and the lag time and maximum slope of these curves were obtained. As shown in Figs. 1 and 3, at physiological pH, heparin and human $Tau_{244-372}$ formed a tight 1:1 complex under reducing conditions, triggering Tau fibrillization. Further fibrillization kinetics analyses showed that the lag time appeared to be approximately invariant up to a molar ratio of 2:1 and then got longer at larger ratios of heparin/Tau in the presence of DTT (Fig. 4*B*). The maximum slope representing the apparent rate constant for fibril growth increased sharply with substoichiometric ratios of heparin/Tau and then decreased to some extent with ratios of >1:1 in the presence of DTT (Fig. 4*A*).

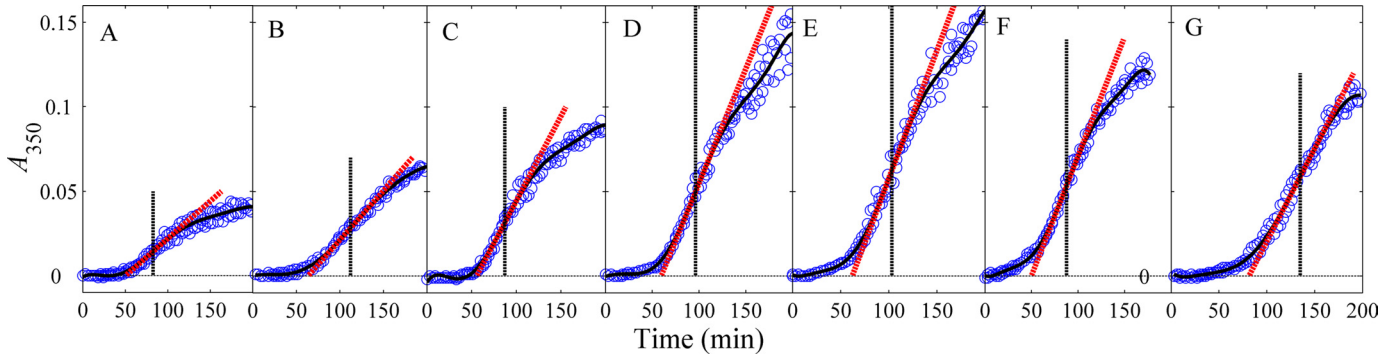

FIGURE 3. **The dependence of turbidity changes for $Tau_{244-372}$ filament formation at 37.0 °C on the molar ratio of heparin to Tau protein.** The concentrations of $Tau_{244-372}$ and DTT were 160 μM and 1 mM, respectively. The molar ratio of heparin to $Tau_{244-372}$ was 1:8 (*A*), 1:6 (*B*), 1:4 (*C*), 1:2 (*D*), 1:1 (*E*), 2:1 (*F*), and 4:1 (*G*), respectively. A seventh order polynomial was fitted to all data (*open circles*) from replicates at each heparin concentration. The kinetic curves were analyzed as described under "Experimental Procedures."

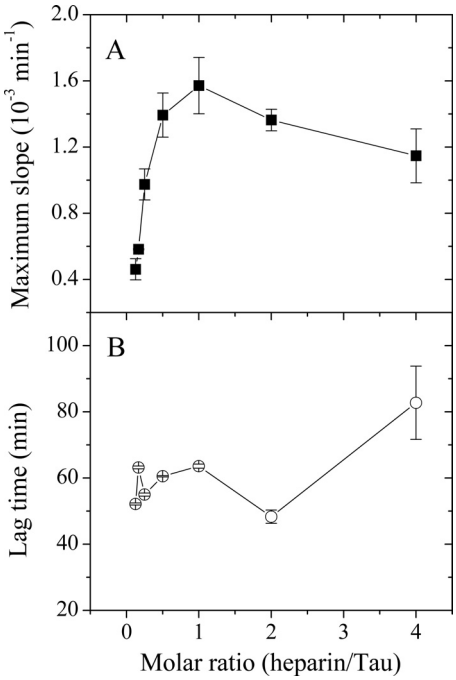

FIGURE 4. **Kinetic analyses for filament formation of $Tau_{244-372}$ as a function of the molar ratio of heparin to Tau protein.** Maximum slope (*A*) and lag time (*B*) changes for filament formation of $Tau_{244-372}$ are shown. The data are expressed as the means ± S.D. (n = 3–4). The temperature was 37.0 °C.

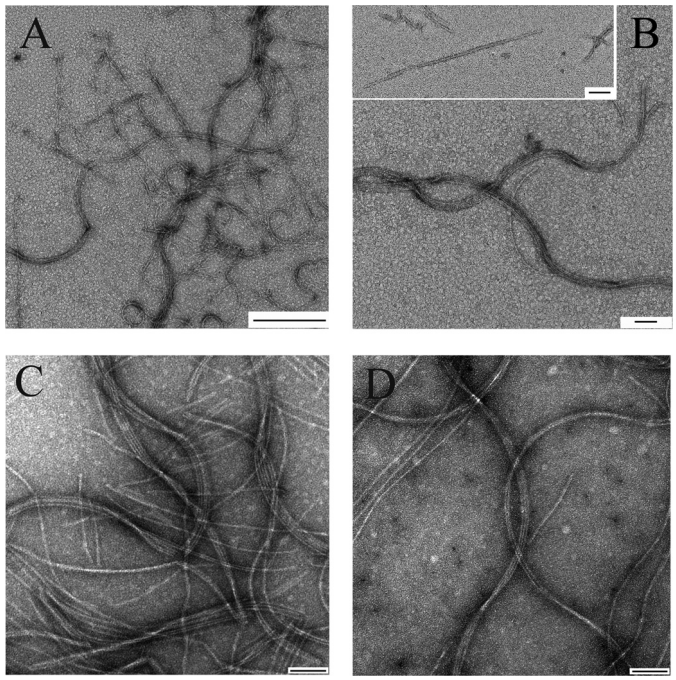

FIGURE 5. **Transmission electron micrographs of $Tau_{244-372}$ samples at physiological pH.** The micrographs shown were created in the presence of 1 mM DTT (*A* and *B*) and in the absence of DTT (*C* and *D*) after incubation for 12 h. Straight filaments formed by $Tau_{244-372}$ in the presence of DTT are shown in the *inset* of *B*. The concentration of $Tau_{244-372}$ was 80 μM and the molar ratio of heparin to $Tau_{244-372}$ was 1:2. A 2% (w/v) uranyl acetate solution was used to negatively stain the fibrils. The *scale bars* in *B–D* represent 100 nm, and that in *A* represents 500 nm.

Heparin-mediated Tau Filament Formation under Oxidative Conditions—To monitor the fibrillization of $Tau_{244-372}$ in the absence of DTT, injection 14 had an 8-h interval after 13 consecutive injections. The ITC curve of the fibrillization of $Tau_{244-372}$ was shown in Fig. 2*C*. The curve represented heat of the reaction as a function of time by integrating the power change (ΔP) peak of the reaction shown in the *inset* box, corrected by the reference. This represented the kinetics of the reaction via the enthalpy production, indicating the high accuracy and low noise of the measurement even without smoothing of the data (Fig. 2*C*, *inset*). The calorimetric data between 60 and 540 min clearly confirmed that heparin mediated Tau filament formation under oxidative conditions (Fig. 2*C*). Meanwhile the transmission electron microscopy image of $Tau_{244-372}$ aggregates formed in the ITC cell showed typical long and branched fibrils, further confirming the fibrillization of $Tau_{244-372}$ induced by heparin (Fig. 2*D*).

Characterization of Morphology of Human Tau Samples—Transmission electron microscopy was used to study the morphology of human Tau samples incubated under different conditions. For wild-type $Tau_{244-372}$, the addition of DTT had no significant effect on the morphology of Tau samples, and long and branched fibrils as well as straight filaments were observed in both samples (Fig. 5), indicating that heparin could induce Tau filament formation under reducing or oxidative conditions.

DISCUSSION

Tau monomers do not assemble spontaneously under physiological conditions over experimentally tractable time periods (20), and Tau fragments cannot assemble spontaneously to

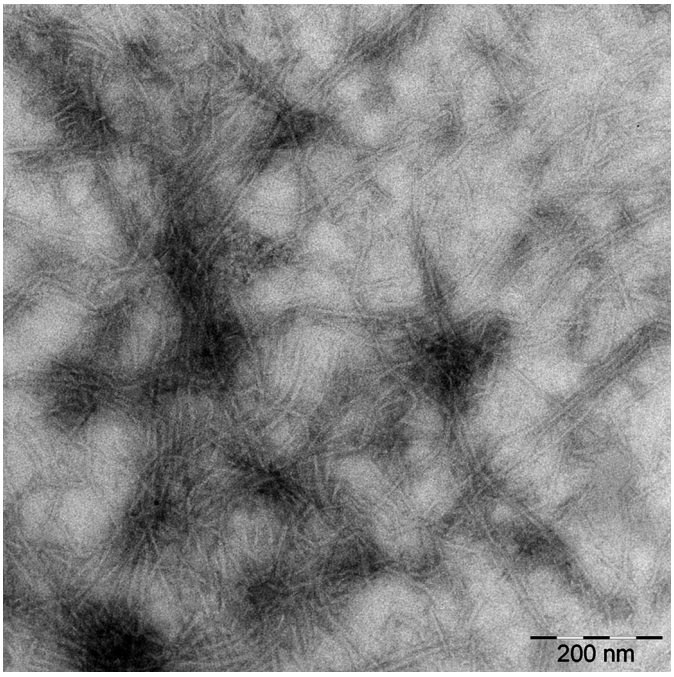

FIGURE 6. **Transmission electron micrograph of full-length human Tau sample at physiological pH in the presence of 2 mM DTT after incubation for 72 h.** The concentration of full-length human Tau protein was 20 μM, and the molar ratio of heparin to Tau was 1:1. A 2% (w/v) uranyl acetate solution was used to negatively stain the fibrils. The *scale bar* represents 200 nm.

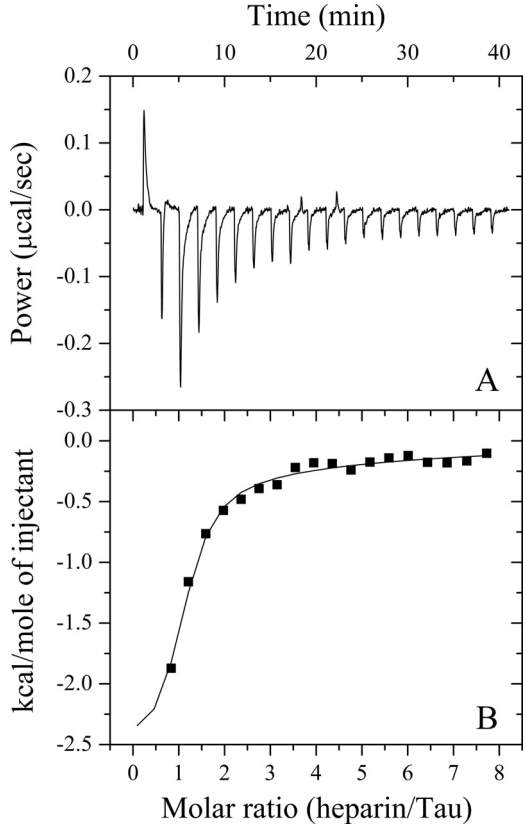

FIGURE 7. **ITC measurements of the binding of heparin to full-length Tau protein at 37.0 °C.** *A* represents typical calorimetric titration of full-length Tau (40 μM) with heparin (1.5 mM) in the absence of DTT. The first injection (0.5 μl) was followed by 19 injections of 2 μl. *B* shows the plots of the heat evolved (kcal) per mol of heparin added, corrected for the heat of heparin, against the molar ratio of heparin to full-length Tau. The data (*solid squares*) were fitted to a two sequential binding sites model and the *solid line* represents the best fit. The ITC machine used here was an iTC_{200} titration calorimetry (MicroCal).

form amyloid filaments over a period of days when the concentration is lower than 150 μM (30, 31). The pathological aggregation of Tau is a nucleation-elongation reaction that involves the formation of β-structure containing some hexapeptide motifs of the repeat domain (21). The "driving force" for filament formation by the Tau repeat domain involves both the formation of an intermolecular disulfide bond (10) and noncovalent interactions such as hydrogen bonds, electrostatic interactions, and hydrophobic interactions (17). Then the elongation can proceed from the nuclei (10).

In the present study, Tau filaments formed within hours when the Tau fragment was incubated with heparin. Polyanionic cofactors, such as heparin and thiazine red, cause structural and conformational changes of Tau protein (17, 32, 33), and then the kinetic and thermodynamic barriers for Tau fibrillization can be overcome (1, 34). Although heparin is not a perfect model for HS, which coexists with Tau protein in nerve cells (12), both heparin and HS induce formation of Tau filaments with very similar morphologies (35). Moreover, the addition of heparin into full-length human Tau protein induces the assembly of Tau into filaments that closely resemble those observed in Alzheimer disease brain tissue (12). Therefore, this study has implications for the putative role of endogenous HS proteoglycans in the formation of neurofibrillary tangles in Alzheimer disease. The extension of the present study of the characterization of heparin binding to human Tau fragment to the quantitative characterization of HS binding to full-length human Tau protein should lead to a better understanding of how HS proteoglycans mediate Tau filament formation in the physiological environment in Alzheimer disease brain.

So far, our experiments were conducted with human Tau fragment, but because filaments in Alzheimer disease contain full-length Tau protein, it is important to demonstrate the behavior of full-length Tau bound by heparin. The human Tau fragment used in this study encompasses the four microtubule-binding repeats, which does exclude a number of domains that could potentially interact with heparin. The main difference is that full-length Tau forms filaments in the presence of heparin much more slowly than $Tau_{244-372}$ induced by heparin (36). However, we did observe straight filaments formed by $Tau_{244-372}$ induced by heparin (Fig. 5), similar to those formed by more complete Tau proteins (12) and by full-length human Tau (Fig. 6) induced by heparin. Our additional ITC experiments (Fig. 7) indicated that in the absence of DTT, heparin bound to full-length human Tau protein with a moderate affinity ($2.38 \times 10^5\ M^{-1}$) at the first binding site followed by one weak binding event ($2.80 \times 10^3\ M^{-1}$). Clearly, the binding affinity of heparin to full-length human Tau at the first binding site closely resembles that of heparin to $Tau_{244-372}$. Based on our results and the recently published data (17), we suggest that heparin binds to full-length human Tau mainly through its segment 244–372, forming the 1:1 complex and triggering Tau fibrillization.

Neuronal cells normally have a reducing environment maintained by an excess of glutathione (1, 8). In this study, DTT, a

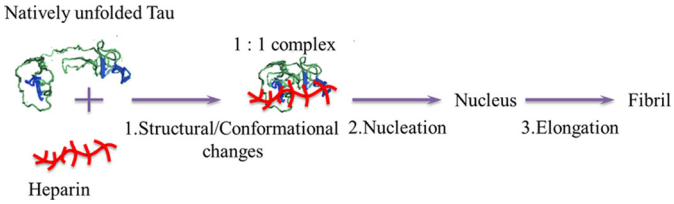

FIGURE 8. **Hypothetical model for heparin-mediated Tau filament formation at physiological pH.** The first step is the interaction of heparin (*red branched structure*) with the natively unfolded Tau protein (*ribbon diagram* in *color*), forming a 1:1 complex and inducing structural and conformational changes of Tau protein, and then the nuclei are formed, which is the rate-limiting step, followed by the step of fibril elongation. Regions of β-structure are shown in *blue*.

strong reducing agent, was used to mimic the reducing environment present in normal neuronal cells. Our data here clearly showed that at physiological pH, heparin 7K and human Tau fragment formed a tight 1:1 complex under physiological reducing conditions, triggering Tau fibrillization. High affinity binding of heparin to Tau protein under reducing conditions provides the necessary charge compensation to allow fibril growth (17). An oxidative (without DTT present plus air oxidation) experimental condition is closer to the physiological environment in Alzheimer disease brain (31, 37). Our ITC data demonstrated that heparin bound to Tau fragment with a moderate binding affinity under pathological oxidative conditions, similarly triggering Tau fibrillization. Kardos and co-workers (38) have reported the first ITC study of amyloid formation, *e.g.* the seed-dependent extension of β_2-microglobulin amyloid fibrils under acidic conditions. Here, we report for the first time a direct thermodynamic study of the interaction between amyloidogenic protein and inducer as well as inducer-triggered fibril formation using ITC.

Our time-dependent turbidity measurements revealed that the lag time did not vary significantly, but the apparent rate constant for the growth of fibrils increased sharply as the molar ratio of heparin to Tau increased up to 1:1 under reductive conditions, suggesting that heparin plays a regulatory role mainly in the elongation process of Tau fibrillization. When the molar ratio of heparin to Tau exceeded unity, the lag time increased, and the apparent rate constant of fibril growth decreased to some extent. The retarding effect of excess heparin is attributed to a large increase in ionic strength of the medium arising from excess unbound heparin (13, 39), which was confirmed by control experiments at fixed heparin concentrations and increasing salt concentrations (supplemental Fig. S1).

Based on our kinetic and thermodynamic data and the recently reported results (17, 33, 34, 39, 40), we propose a valuable hypothesis for heparin-mediated Tau filament formation that the first step of kinetics involves binding of heparin to the natively unfolded Tau protein, forming a 1:1 complex and inducing structural and conformational changes of Tau protein, and then the nuclei are formed, which is the rate-limiting step, followed by the step of fibril elongation at physiological pH (Fig. 8). The hypothesis proposed here is different from the previous hypothesis (33) in the following aspects. First, we propose that the binding of heparin (or another polyanion) to monomeric Tau is a prerequisite for the growth of Tau fibrils. Second, we speculate that the binding of heparin to Tau monomer induces conformational changes in Tau, as well as reducing the large net positive charge borne by Tau protein, thus reducing the activation energy required to add Tau to the end of a growing Tau fiber and accelerating fibril growth. Therefore the formation of a 1:1 complex of Tau monomer and heparin plays an important role in the inducer-mediated Tau filament formation, providing clues to understanding the pathogenesis of neurodegenerative diseases.

Acknowledgments—We sincerely thank Dr. Michel Goedert (Laboratory of Molecular Biology, Medical Research Council, Cambridge, UK) for kindly providing the plasmid for human Tau40 and Prof. Guang-Fu Yang (College of Chemistry, Central China Normal University, Wuhan, China) for technical assistance with iTC$_{200}$.

REFERENCES

1. Kuret, J., Chirita, C. N., Congdon, E. E., Kannanayakal, T., Li, G., Necula, M., Yin, H., and Zhong, Q. (2005) *Biochim. Biophys. Acta* **1739,** 167–178
2. Skovronsky, D. M., Lee, V. M., and Trojanowski, J. Q. (2006) *Annu. Rev. Pathol.* **1,** 151–170
3. Braak, H., and Braak, E. (1997) *Neurobiol. Aging* **18,** 351–357
4. Goedert, M. (1993) *Trends Neurosci.* **16,** 460–465
5. Gómez-Isla, T., Hollister, R., West, H., Mui, S., Growdon, J. H., Petersen, R. C., Parisi, J. E., and Hyman, B. T. (1997) *Ann. Neurol.* **41,** 17–24
6. Aoyagi, H., Hasegawa, M., and Tamaoka, A. (2007) *J. Biol. Chem.* **282,** 20309–20318
7. Mandelkow, E., Song, Y. H., Schweers, O., Marx, A., and Mandelkow, E. M. (1995) *Neurobiol. Aging* **16,** 347–354
8. Rosenberg, K. J., Ross, J. L., Feinstein, H. E., Feinstein, S. C., and Israelachvili, J. (2008) *Proc. Natl. Acad. Sci. U.S.A.* **105,** 7445–7450
9. Wille, H., Drewes, G., Biernat, J., Mandelkow, E. M., and Mandelkow, E. (1992) *J. Cell Biol.* **118,** 573–584
10. Friedhoff, P., von Bergen, M., Mandelkow, E. M., Davies, P., and Mandelkow, E. (1998) *Proc. Natl. Acad. Sci. U.S.A.* **95,** 15712–15717
11. Pérez, M., Valpuesta, J. M., Medina, M., Montejo de Garcini, E., and Avila, J. (1996) *J. Neurochem.* **67,** 1183–1190
12. Goedert, M., Jakes, R., Spillantini, M. G., Hasegawa, M., Smith, M. J., and Crowther, R. A. (1996) *Nature* **383,** 550–553
13. Friedhoff, P., Schneider, A., Mandelkow, E. M., and Mandelkow, E. (1998) *Biochemistry* **37,** 10223–10230
14. Chirita, C. N., and Kuret, J. (2004) *Biochemistry* **43,** 1704–1714
15. Kampers, T., Friedhoff, P., Biernat, J., Mandelkow, E. M., and Mandelkow, E. (1996) *FEBS Lett.* **399,** 344–349
16. Wilson, D. M., and Binder, L. I. (1997) *Am. J. Pathol.* **150,** 2181–2195
17. Sibille, N., Sillen, A., Leroy, A., Wieruszeski, J. M., Mulloy, B., Landrieu, I., and Lippens, G. (2006) *Biochemistry* **45,** 12560–12572
18. Ferrone, F. (1999) *Methods Enzymol.* **309,** 256–274
19. Necula, M., and Kuret, J. (2004) *Anal. Biochem.* **333,** 205–215
20. Chirita, C. N., Congdon, E. E., Yin, H., and Kuret, J. (2005) *Biochemistry* **44,** 5862–5872
21. Barghorn, S., Biernat, J., and Mandelkow, E. (2005) *Methods Mol. Biol.* **299,** 35–51
22. van Holde, K. E., Johnson, W. E., and Ho, P. S. (2006) *Principles of Physical Biochemistry*, pp. 91–93, Pearson Prentice Hall, Upper Saddle River, NJ
23. Theisen, A., Deacon, M. P., Johann, C., and Harding, S. E. (2000) *Refractive Increment Data-book: For Polymer and Biomolecular Scientists*, p. 55, Nottingham University Press, Nottingham, UK
24. Pavlov, G., Finet, S., Tatarenko, K., Korneeva, E., and Ebel, C. (2003) *Eur. Biophys. J.* **32,** 437–449
25. Attri, A. K., and Minton, A. P. (2005) *Anal. Biochem.* **346,** 132–138
26. Kameyama, K., and Minton, A. P. (2006) *Biophys. J.* **90,** 2164–2169
27. Stacey, K. A. (1956) *Light Scattering in Physical Chemistry*, Academic Press, New York

28. Liang, Y., Du, F., Sanglier, S., Zhou, B. R., Xia, Y., Van Dorsselaer, A., Maechling, C., Kilhoffer, M. C., and Haiech, J. (2003) *J. Biol. Chem.* **278,** 30098–30105
29. Xu, H., Liang, Y., Zhang, P., Du, F., Zhou, B. R., Wu, J., Liu, J. H., Liu, Z. G., and Ji, L. N. (2005) *J. Biol. Inorg. Chem.* **10,** 529–538
30. Goux, W. J., Kopplin, L., Nguyen, A. D., Leak, K., Rutkofsky, M., Shanmuganandam, V. D., Sharma, D., Inouye, H., and Kirschner, D. A. (2004) *J. Biol. Chem.* **279,** 26868–26875
31. Schweers, O., Mandelkow, E. M., Biernat, J., and Mandelkow, E. (1995) *Proc. Natl. Acad. Sci. U.S.A.* **92,** 8463–8467
32. Paudel, H. K., and Li, W. (1999) *J. Biol. Chem.* **274,** 8029–8038
33. Congdon, E. E., Kim, S., Bonchak, J., Songrug, T., Matzavinos, A., and Kuret, J. (2008) *J. Biol. Chem.* **283,** 13806–13816
34. Carlson, S. W., Branden, M., Voss, K., Sun, Q., Rankin, C. A., and Gamblin, T. C. (2007) *Biochemistry* **46,** 8838–8849
35. Hasegawa, M., Crowther, R. A., Jakes, R., and Goedert, M. (1997) *J. Biol. Chem.* **272,** 33118–33124
36. Barghorn, S., and Mandelkow, E. (2002) *Biochemistry* **41,** 14885–14896
37. Smith, C. D., Carney, J. M., Starke-Reed, P. E., Oliver, C. N., Stadtman, E. R., Floyd, R. A., and Markesbery, W. R. (1991) *Proc. Natl. Acad. Sci. U.S.A.* **88,** 10540–10543
38. Kardos, J., Yamamoto, K., Hasegawa, K., Naiki, H., and Goto, Y. (2004) *J. Biol. Chem.* **279,** 55308–55314
39. Jeganathan, S., von Bergen, M., Mandelkow, E. M., and Mandelkow, E. (2008) *Biochemistry* **47,** 10526–10539
40. von Bergen, M., Barghorn, S., Müller, S. A., Pickhardt, M., Biernat, J., Mandelkow, E. M., Davies, P., Aebi, U., and Mandelkow, E. (2006) *Biochemistry* **45,** 6446–6457